

See discussions, stats, and author profiles for this publication at:
<https://www.researchgate.net/publication/239160542>

Formation energetics of n-member rings at the end of small zigzag carbon nanotubes

ARTICLE *in* CHEMICAL PHYSICS LETTERS · MAY 2002

Impact Factor: 1.9 · DOI: 10.1016/S0009-2614(02)00594-8

CITATIONS

2

READS

13

5 AUTHORS, INCLUDING:



Renchao Che

Fudan University

118 PUBLICATIONS 3,121 CITATIONS

SEE PROFILE



Lian-Mao Peng

Peking University

394 PUBLICATIONS 9,688 CITATIONS

SEE PROFILE



Shansahn Zhang

Shanxi Normal University

749 PUBLICATIONS 12,660 CITATIONS

SEE PROFILE



Shuzhi Wang

Chinese Academy of Social Sciences

1,222 PUBLICATIONS 19,462 CITATIONS

SEE PROFILE

Formation energetics of n -member rings at the end of small zigzag carbon nanotubes

R. Che ^a, L.-M. Peng ^{b,a,*}, S. Zhang ^b, S. Wang ^b, J. Luo ^b

^a *Beijing Laboratory of Electron Microscopy, Institute of Physics and Center for Condensed Matter Physics, Chinese Academy of Sciences, P.O. Box 2724, Beijing 100080, China*

^b *Department of Electronics, Peking University, Beijing 100871, China*

Received 31 January 2002; in final form 5 April 2002

Abstract

The formation energetics and stability of n -member rings at the end of small zigzag carbon nanotubes are investigated using k -space tight-binding molecular dynamics simulations (TBMDs). It is found that at 1100 °C the initial dangling atoms at the end of a small $(n,0)$ zigzag carbon nanotube can transform into an n -member ring if the tube is larger than a $(3,0)$ tube but smaller than a $(11,0)$ tube. For zigzag tubes larger than $(10,0)$ the large strain associated with the n -member ring prevents the formation of the ring at the end of the tube. It is shown that the 6-member ring formed at the top of a $(6,0)$ tube is the most stable one, and that the formation of the ring at the top of small zigzag tubes may introduce new ring states around the Fermi level. © 2002 Published by Elsevier Science B.V.

1. Introduction

Since the discovery of carbon nanotubes (CNTs) by Iijima in 1991 [1], different models have been put forward to explain the growth of CNTs [2–8]. For nanotubes with closed ends, it was proposed that C_2 dimers or small carbon clusters may be incorporated around the pentagon–heptagon pairs at the closed ends through Stone–Wales mechanism [9,10] so as to continue longitudinal growth. On the other hand for nanotubes with open ends, the growth of CNTs was believed

to be via the addition of C_2 dimers and C_3 trimers at the open ends and the making of new bonds with the active dangling atoms at the open ends [11,12]. The key question concerning the growth of CNTs is whether or not an open-ended CNT will remain open during the growth process [13]. It was estimated that the formation of the tube closure is energetically favorable only for tubes narrower than a critical diameter of about 3 nm [14]. In this Letter we will show, via tight-binding molecular dynamics simulations (TBMDs), that the critical diameter depends indeed on the growth temperature. At 1100 °C, which lies at the upper end of the temperature range used in a typical chemical vapor deposition (CVD) experiment, dangling atoms (i.e., those with dangling bonds) at the end of small $(n,0)$ zigzag carbon nanotubes can bond together

* Corresponding author. Fax: +86-10-6256-1422.

E-mail addresses: plm@ele.pku.edu.cn, lian-mao.peng@physics.org (L.-M. Peng).

along the circumferential direction and form an n -member ring, and the n -member ring is mechanically stable for tubes that are larger than a (3,0) tube but smaller than a (11,0) tube.

2. Methods

Our molecular dynamics (MD) simulations are performed using the OXON code [15] which is based on the orthogonal tight-binding (TB) method and the local charge neutrality approximation [16,17]. For small hydrocarbons as well as polyacetylene isomers, the TB method produces results which agree well with experimental values and the more accurate ab initio results [18]. Because large scale single-walled carbon nanotubes (SWCNTs) can be synthesized under CVD condition [19], we carried out all our MD calculations at 1100 °C. The time step used in all MD calculation is 1 fs.

A geometric model for a general (n, m) carbon nanotube was first constructed by rolling up a two-dimension sheet of graphite assuming a C–C bond length of 0.142 nm, and the tube is specified uniquely by the chiral vector $\mathbf{C}_h = n\mathbf{a}_1 + m\mathbf{a}_2$. In this Letter we will discuss only zigzag tubes with $m = 0$, i.e., $(n, 0)$ tubes, and a typical atomic model is shown in Fig. 1. In the TB model, the total binding energy may be written as [15,16]

$$U_{\text{binding}} = 2 \sum_{i\alpha \neq j\beta} \rho_{j\beta, i\alpha} H_{i\alpha, j\beta} + \frac{1}{2} \sum_{i \neq j} \phi(r_{ij}) + \sum_{i\alpha} [2\rho_{i\alpha, i\alpha} - N_{i\alpha}^{\text{atom}}] \varepsilon_{i\alpha}, \quad (1)$$

where i and j are indices of atoms, α and β are indices of atomic orbitals (2s, 2p_x, 2p_y, 2p_z), $\rho_{i\alpha, j\beta}$ and $H_{i\alpha, j\beta}$ are the density and Hamiltonian matrix elements between two atomic orbitals with indices $i\alpha$ and $j\beta$, $\phi(r_{ij})$ is a pairwise repulsive potential between atoms i and j , $N_{i\alpha}^{\text{atom}}$ denotes the occupancy of the α th atomic orbital of the i th atom and $\varepsilon_{i\alpha}$ denotes the corresponding energy level when the atom is free. Physically, the first term on the right-hand-side of Eq. (1) represents the bond energy contribution, the second term denotes the repulsive energy contribution and the third term

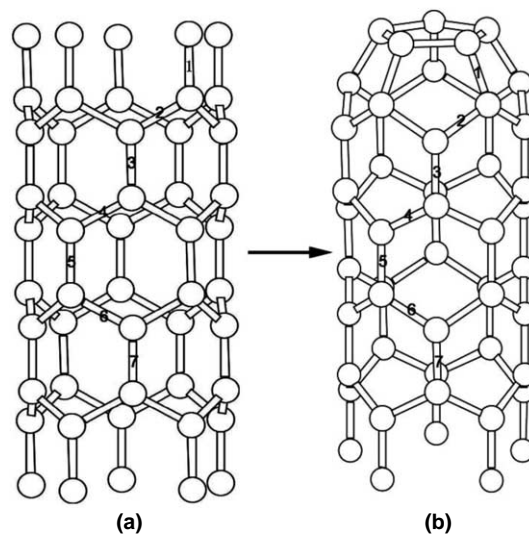


Fig. 1. (a) Atomic model and (b) a snapshot of a (5,0) tube resulting from MD simulation at $T = 1373$ K: MD simulations were made with the lower end of the tube fixed, and the snapshot is obtained at 800 fs. Seven bonds are marked in the figure by 1, 2, 3, 4, 5, 6 and 7; among which bonds marked by 1, 3, 5 and 7 are oriented parallel to the tube axis and those marked by 2, 4, 6 make an angle of 60° with the tube axis.

the promotion energy contribution. The total force acting on an atom may be accordingly decomposed into Hellmann–Feynman forces due to bond energy, short range repulsive forces and forces resulting from promotion energy [16,17,20]

$$\vec{F}_k = - \left(\frac{\partial U_{\text{binding}}}{\partial \vec{r}_k} \right) = -2 \sum_{i\alpha \neq j\beta} \rho_{j\beta, i\alpha} \left(\frac{\partial H_{i\alpha, j\beta}}{\partial \vec{r}_k} \right) - \left(\frac{1}{2} \right) \sum_{i \neq j} \left(\frac{\partial \phi(r_{ij})}{\partial \vec{r}_k} \right) - \sum_{i\alpha} (2\rho_{i\alpha, i\alpha} - N_{i\alpha}^{\text{atom}}) \left(\frac{\partial \varepsilon_{i\alpha}}{\partial \vec{r}_k} \right). \quad (2)$$

At finite temperature the atomic trajectories may be obtained via MD procedure, while the ground state structure or equilibrium structure of the carbon nanotube may be obtained via minimizing the forces acting on the atoms or alternatively the total energy of the system. It is found that structural relaxation introduces hardly any significant changes to the geometric model of a zigzag tube.

3. Results and discussion

Shown in Fig. 1 are two snapshots of a (5,0) carbon nanotube from a MD simulation performed at 1100 °C. The initial atomic model used for the MD simulation is shown in Fig. 1a. From this model we see that there exist two types of bond in a zigzag nanotube: one orients parallel to the tube axis, which we call axis-oriented bonds; and the other makes a 60° angle with the tube axis, which we call circumference-oriented bonds. At the top end of the model there exist five dangling atoms making bonds of type 1 with the atoms beneath them at the second layer. During MD process, the five dangling atoms adjust themselves toward the tube axis along the radial direction and form a pentagon at the top of the tube accompanied by five neighboring pentagons after 800 MD steps, i.e., at 800 fs. Similar transformation was found for all (*n*, 0) tubes with *n* ranging from 4 to 10, i.e., the initial *n* dangling atoms at the top end of an (*n*, 0) tube became bonded together forming an *n*-member ring of *C_n* site symmetry about the tube axis at the top of the tube and *n* accompanying pentagons with the *n* atoms of the second layer. For zigzag tubes larger than a (10,0) tube, the top *n* dangling atoms failed to form an *n*-member ring. Instead some isolated C₂ dimers were formed among the initial dangling atoms leaving the top of the tube basically an open end.

Shown in Fig. 2 are changes of seven bond lengths after MD relaxation for the selected seven C–C bonds of the (5,0) tube as shown in Fig. 1. The four axis-oriented bonds are 1, 3, 5, 7 and the remaining three 2, 4, 6 are circumference-oriented bonds making angles of about 60° with the tube axis. After the formation of the pentagon at the top end of the (5,0) tube, the tube becomes closed at the end. Bond lengths of all axis-oriented bonds such as bonds 1, 3, 5 and 7 are increased, while bond lengths of all circumference-oriented bonds

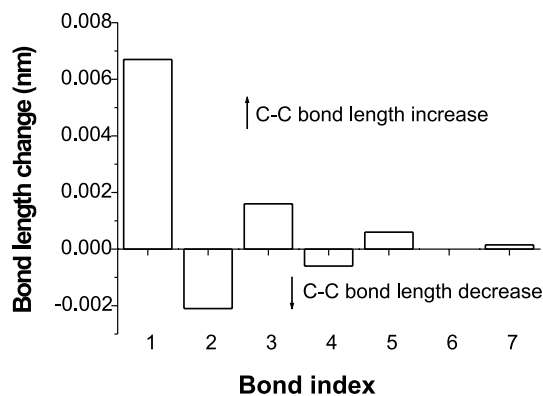


Fig. 2. Bond length changes for the seven marked bonds of Fig. 1 after MD relaxation.

are decreased (see Table 1 for numerical values) so that the total change in the volume of the tube is reduced to a minimum level. Because a zigzag tube has a *C_n* symmetry about the tube axis, the change of one bond represents indeed the change of all other bonds of the same type. It can also be seen from Fig. 2 that the bond length shows oscillating behavior with the distance away from the top pentagon and the amplitude of oscillation decays with the distance and the bond length converges to that of the bulk bond at about four to five layers of atoms.

Shown in Fig. 3 are the bond energy changes for the marked seven bonds of Fig. 1. Here the bond energy change ΔE_{ij} for a particular bond between atoms *i* and *j* is defined using Eq. (1) as

$$\Delta E_{ij} = 2 \left(\sum_{ix,j\beta \neq ix} H_{ix,j\beta} \rho_{j\beta,ix} \right)_{\text{after MD}} - 2 \left(\sum_{ix,j\beta \neq ix} H_{ix,j\beta} \rho_{j\beta,ix} \right)_{\text{before MD}},$$

which reflects whether a bond is weakened ($\Delta E_{ij} < 0$) or strengthened ($\Delta E_{ij} > 0$). The trend

Table 1
Bond length and energy changes for several bonds as marked in Fig. 1

Bond index	1	2	3	4	5	6	7
Bond length change (nm)	0.0067	−0.0021	0.0016	−0.0006	0.0006	0	0.00015
Bond energy change (eV)	3.072	−0.949	0.523	−0.491	0.025	−0.283	0.004

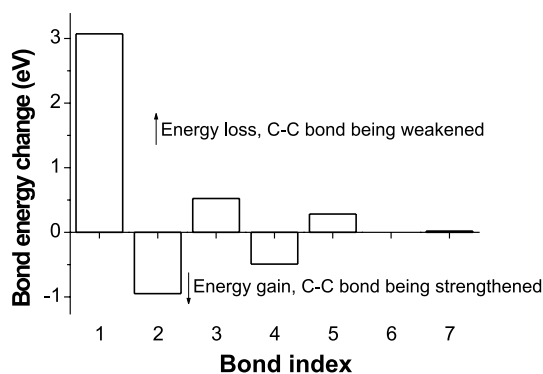


Fig. 3. Bond energy changes for the seven marked bonds of Fig. 1 after MD relaxation.

of the bond energy variation shown in Fig. 3 is consistent with the trend shown in Fig. 2 by the bond length. For example, the length of bond 3 of Fig. 3b increased 0.0016 nm with respect to Fig. 1a, and the bond energy of the same bond decreased by about 0.523 eV. The length of bond 4 decreased 0.0006 nm, and the corresponding bond energy increased 0.491 eV. In general for an $(n, 0)$ zigzag tube with $3 < n < 11$, after the formation of the n -member ring at the top end of the tube, all axis-oriented bonds are weakened with increased bond length while all circumference-oriented bonds are strengthened with reduced bond length.

The n -member rings formed at the top of zigzag nanotubes with index ranging from (4,0) to (10,0) are square, pentagon, hexagon, heptagon, octagon, enneagon and decagon, respectively. For all the tube modes considered in this Letter, we used the same tube length of 2.5 nm. To understand the stability of the nanotubes and the n -member rings formed at the top end of these tubes, we divide the total energy gain from MD relaxation $\Delta U_{\text{binding}}$ by the total number of atoms of the tube N and write

the total binding energy as the sum of bond energy, promotion energy and repulsive energy [21] as in Eq. (1). We calculate the total binding energy per atom, i.e., U_{binding}/N , for each tube before and after MD relaxation, and define the energy gain per atom $\Delta U_{\text{binding}}/N$ being the difference between the two binding energies of the tube after and before MD relaxation.

Listed in Table 2 are total energy gains for some zigzag tubes after the formation of the n -member rings at the top of these tubes. It is shown that initially the energy gain (per atom) increases as the tube diameter increases from (4,0) tube to (6,0) tube, and then the energy gain decreases monotonically from (6,0) tube to (10,0) tube. The largest energy gain per atom occurs for the (6,0) tube with $\Delta E = -0.181$ eV when a perfect hexagon is formed at the top of the tube, while for the (11,0) tube the dangling atoms failed to form an n -member ring like smaller tubes. Instead several isolated dimers are formed among the dangling atoms and the total energy is reduced by 0.089 eV per atom as the result of the dimers formation. Although the n -member ring cannot be formed automatically via MD relaxation, we can nevertheless construct the ring geometrically adapting the geometry and parameters obtained from smaller tubes. Table 2 shows that the geometrically constructed (11,0) tube will loss energy by as much as 0.035 eV per atom and the same picture is found for other larger tubes, i.e., the formation of the n -member ring is energetically not favorable for zigzag tubes with a diameter larger than that of a (10,0) tube.

Table 2 may be understood by considering two competing factors associated with the formation of the n -member ring. On the one hand, the formation of the n -member ring may effectively eliminate

Table 2
Total energy gain for some zigzag $(n, 0)$ tubes

Tube index	(4,0)	(5,0)	(6,0)	(7,0)	(8,0)	(9,0)	(10,0)	(11,0) _I	(11,0) _{II}
Total energy gain per atom (eV)	-0.150	-0.162	-0.181	-0.146	-0.144	-0.136	-0.127	-0.086	0.035
Total number of atoms N	40	50	60	70	80	90	100	110	110
Total energy gain (eV)	-6.00	-8.10	-10.86	-10.22	-11.52	-12.24	-12.70		
Total energy gain per bond (eV)	-1.50	-1.62	-1.81	-1.46	-1.41	-1.36	-1.27		

* (11,0)_I – (11,0) tube with isolated dimers; (11,0)_{II} – (11,0) tube with 11-member ring.

dangling bonds associated with the dangling atoms and therefore reduce the total binding energy of the system. On the other hand, in order to form an n -member ring at the top of a zigzag tube, all atoms at the top end of the tube must move away from their ideal geometric positions and introduce distortion to bond angles and introduce strain to the system. To make the above argument more quantitatively, we calculated the bond energy of all zigzag tubes with $3 < n < 12$ and divided all C–C bonds into three groups: ring bonds associated with the top n -member ring, axis-oriented bonds and circumference-oriented bonds as defined before. The bond energy gain per atom for each tube is calculated separately for the three groups of bonds and shown in Fig. 4, i.e., those resulting from the new bonds associated with the n -member ring, and those from the axis-oriented and circumference-oriented bonds. The trend shown by the axis-oriented bond group and n -member ring bond group are straightforward, i.e., the more atoms in the n -member ring the larger the bond energy gain (as a result of the reduction of the dangling bonds), the larger the tube the higher the strain energy (simply because all axis-oriented bonds are elongated as a result of the formation of the n -member ring). The circumference-oriented bond group, on the other hand, exhibits a more complicated behavior. For the smallest (4,0) tube considered here the four-member ring is a square having higher strain energy than that associated

with a larger (5,0) tube having a five-member pentagon ring. The strain associated with the circumference-oriented bond group reduces to its minimum when a hexagon is formed at the top end of a (6,0) tube, and then increases monotonically as more and more atoms are involved in the ring until (11,0) tube when the energy gain resulting from the reduction of the dangling bonds is not large enough to compensate for the increase in the strain energy. The conclusion to be drawn from here based on the analysis of the bond energy is the same as from Table 2 based on the total energy, i.e., the formation of the n -member ring with n being bigger than 10 is not energetically favorable.

It is generally believed that topological defects locally introduced into carbon tubes may open a new road toward device applications [20]. An interesting question concerning the formation of the n -member ring at the end of zigzag tubes is how the n -member ring influences the electronic property of the tube. Shown in Fig. 5a are integrated local density of states (ILDOS) for a dangling atom and a bulk atom for a zigzag semiconducting (8,0) tube. The dangling and bulk atoms show very different response to the formation of the n -member ring at the end of the tube. Before MD relaxation, the Fermi level of the tube is -6.55 eV. After MD relaxation, the Fermi level shifts toward lower energy side and becomes -6.79 eV (see Fig. 5b). We note that energy states between -32 eV and -12 eV are mainly associated with the σ bonding states, while that between -10 eV to the Fermi level are mainly associated with the π bonding states. Before MD relaxation, a dangling atom can accommodate only one σ electron and this is manifested by the fact that the value of ILDOS for the dangling atom before MD is less than 0.5 for energy up to -10 eV. After the formation of the n -member ring, two more σ bonds are formed between the initial dangling atom and its two neighbors in the n -member ring and the corresponding value of ILDOS becomes 1.5 at energy around -12 eV. After the formation of the n -member ring, both σ and π states shift toward lower energy side, and the whole tube structure is therefore more stable than that without the n -member ring. Shown in Fig. 5b are local density of

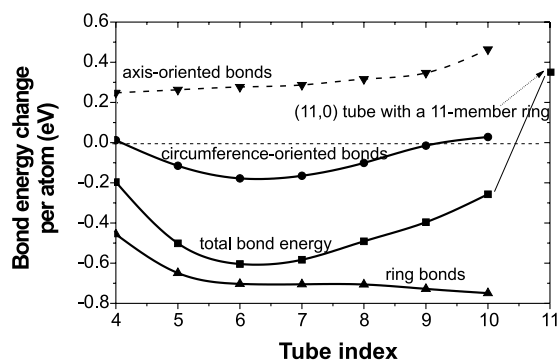


Fig. 4. Bond energy gain per atom (denoted as total in the figure) decomposed into three components resulting from (a) ring bonds, (b) axis-oriented bonds and (c) circumference-oriented bonds.

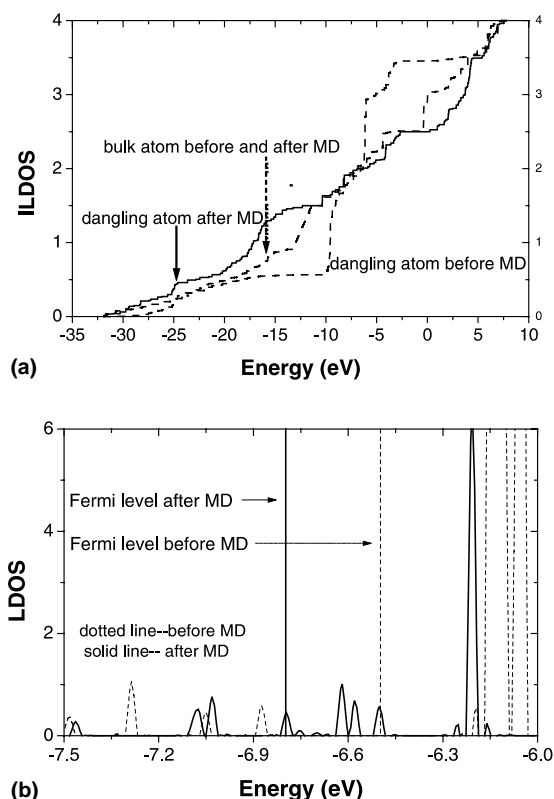


Fig. 5. (a) Integrated local density of states (ILDOS) and (b) local density of states (LDOS) for an end dangling atom at the end of a (8,0) tube before and after MD relaxation.

states (LDOS) curves for a dangling atom. For a geometrically constructed tube, there exists a small energy gap between -6.9 and -6.2 eV, i.e., the tube is a semiconductor tube with no states around the Fermi level at -6.55 eV. After the formation of the n -member ring, new states are introduced around the Fermi level at -6.79 eV, and detailed calculations reveal that the ring states may extend several layers of atoms into the tube. It is expected that these ring states may modify the electronic property of nanotubes to certain extent.

4. Conclusions

In conclusion, we have presented an investigation on the energetics and stability of the dangling atoms at the top end of zigzag nanotubes.

Dangling atoms at the top of a small zigzag nanotube with its index lying between (4,0) and (10,0) will bond together automatically during MD relaxation at 1100 °C and form an n -member ring at the end. The total energy gain per atom for a (6,0) tube is the largest among these small zigzag tubes, because the strain associated with the formation of a perfect six-member hexagon ring at the end of the (6,0) tube reduces to the minimum. For zigzag tubes with their diameter larger than that of a (10,0) tube, the energy gain resulting from the reduction of the dangling bonds of the end dangling atoms is not sufficient to compensate the energy loss resulting from the increase of strain energy, the formation of the n -member ring at the ends of these tubes is energetically not favorable. The formation of the n -member ring may introduce new ring states around the Fermi level. We believe that our findings may have implications on the understanding of the growth process and also on the property modification of carbon nanotubes.

Acknowledgements

This work was supported by the Ministry of Science and Technology of China (Grant No. 001CB610502), Chinese Academy of Sciences and the Royal Society for a joint project that enables one of the authors (L.M.P.) to visit Professor David G. Pettifor at Oxford and bring the OXON code back to Beijing.

References

- [1] S. Iijima, *Nature* 354 (1991) 56.
- [2] J.C. Charlier, A. Devita, X. Blase, R. Car, *Science* 275 (1997) 646.
- [3] M.S. Dresselhaus, G. Dresselhaus, R. Saito, *Phys. Rev. B* 45 (1992) 6234.
- [4] D.L. Carroll, P. Redlich, P.M. Ajayan, J.C. Charlier, X. Blase, A. Devita, *Phys. Rev. Lett.* 78 (1997) 2811.
- [5] S.B. Sinnott, R. Andrew, D. Qian, A.M. Rao, Z. Mao, E.C. Dickey, *Chem. Phys. Lett.* 315 (1999) 25.
- [6] M. Terrones, H. Terrones, F. Banhart, J.C. Charlier, P.M. Ajayan, *Science* 288 (2000) 1226.
- [7] J.C. Charlier, A. Devita, X. Blase, R. Car, *Science* 275 (2000) 647.

- [8] Y.L. Lee, S.G. Kim, D. Tomanek, *Phys. Rev. Lett.* 78 (1997) 2393.
- [9] A. Maiti, C.J. Brabec, J. Bernholc, *Phys. Rev. B* 55 (1997) 6097.
- [10] R. Saito, M. Fujita, G. Dresselhaus, M.S. Dresselhaus, *Mater. Sci. Eng. B* 19 (1993) 185.
- [11] A. Maiti, C.M. Roland, J. Bernholc, *Phys. Rev. Lett.* 73 (1996) 2468.
- [12] S. Iijima, T. Ichihashi, Y. Ando, *Nature* 356 (1992) 776.
- [13] P.M. Ajayan, T.W. Ebbesen, *Rep. Prog. Phys.* 60 (1997) 1025.
- [14] C.J. Brabec, A. Maiti, C. Roland, J. Bernholc, *Chem. Phys. Lett.* 236 (1996) 150.
- [15] A.P. Horsfield, P.D. Godwin, D.G. Pettifor, A.P. Sutton, *Phys. Rev. B* 54 (1996) 15773.
- [16] A.P. Sutton, M.W. Finnis, D.G. Pettifor, Y. Ohta, *J. Phys. C* 21 (1988) 35.
- [17] C.H. Xu, C.Z. Wang, C.T. Chan, K.M. Ko, *J. Phys. Condens. Matter* 4 (1992) 6047.
- [18] P.D. Doodwin, A.P. Horsfield, D.G. Pettifor, A.P. Sutton, *Phys. Rev. B* 54 (1996) 15776.
- [19] H. Dai, J. Kong, C. Zhou, N. Franklin, T. Tombler, A. Cassell, S. Fan, *J. Phys. Chem. B* 103 (1999) 11246.
- [20] V.H. Crespi, M.L. Cohen, *Phys. Rev. Lett.* 79 (1997) 2093.
- [21] D.G. Pettifor, I.I. Oleinik, *Phys. Rev. B* 59 (1999) 8487.